Journal of Molecular Modeling (2020) 26: 96
https://doi.org/10.1007/s00894-020-04367-8

ORIGINAL PAPER

The topology impact on hydrogen storage capacity of Sc-decorated ever-increasing porous graphene

Fatemeh Yasareh[1] · Ali Kazempour[2,3] · Reza Behjatmanesh-Ardakani[1]

Received: 18 September 2019 / Accepted: 25 March 2020 / Published online: 7 April 2020

Abstract

Hydrogen storage capacity of different scandium (Sc)-decorated topological porous graphene (PG) was examined through density functional theory calculations. PGs were selected considering odd and even topological symmetries. Our calculations demonstrate that the most preferable sites for adsorption of Sc are located on the center of carbon rings on the perimeter of pores of all sizes. This results in stronger polarization and hybridization perpendicular to the surface leading to enhanced binding. Thus, all PGs are suitable for hydrogen storage under surrounded settings. Furthermore, results showed that the adsorption energies of H_2 molecules increased gradually with the size of pores. Analysis of charge density difference showed that the presence of Sc could play an efficient role for stronger adsorption of hydrogen molecules rather than increasing pore sizes. Furthermore, projected densities of states indicate that favorable systems for hydrogen storage are those that have higher overlap of individual states at Fermi level. Compared with H_2 adsorption on pure graphene, injecting topological defect such as hexagon porous and decoration with a transition metal atom such as Sc can effectively create much more conductive states at Fermi energy. Eventually, Sc decoration leads to n-type doping of PGs that help in much easier transportation of charge carriers and desirable storage of H_2 molecules.

Keywords Porous graphene · Hydrogen storage · Scandium-decorated PG systems · Density functional theory (DFT)

Introduction

Given the ever-increasing population growth, reduced fossil fuels, and, more importantly, greenhouse gas emissions, the development of clean energy sources is indispensable [1]. Many developed countries are looking for alternative sources of energy. Among the studied cases, hydrogen has received much attention because of its high abundance, performance, quality, and lacking pollution [2–4]. Despite these advantages, the impossibility of hydrogen storage in environmental conditions has prevented the widespread use of this fuel [5].

In this regard, there are three methods of compression, liquefaction, and storage on a solid bed for the storage of hydrogen [6, 7]. Research has shown that suitable hydrogen adsorption energy for H_2 ranges from −0.2 to 0.7 eV/H_2 for adsorbed and desorbed states in environmental conditions, hence storing hydrogen in a solid bed seems to be the most appropriate method [8, 9].

Various solid matters, such as graphene [5, 10, 11] and silicone [12–15], have been investigated as a solid bed. Graphene is a two-dimensional substance consisting of carbon atoms with a honeycomb form. Because of its excellent properties, high thermal conductivity, and excitability in electrical conductivity, this material has attracted much attention compared with other carbon materials. However, the absorption energy of hydrogen molecule on pure graphene surface is weak [9, 16]. Addition of intermediate metals is an effective way to improve absorption energy [8–13]. Metals that have been studied include alkali metals (AMs) (Li, Na, and K), alkali earth metals (AEMs) (Be, Mg, and Ca), transition metals (TM) (Sc, Ti, and V), and a simple metal (Al).

Electronic supplementary material The online version of this article (https://doi.org/10.1007/s00894-020-04367-8) contains supplementary material, which is available to authorized users.

✉ Ali Kazempour
kazempour@pnu.ac.ir

[1] Department of Chemistry, Payame Noor University, P.O. Box 119395-3697, Tehran, Iran

[2] Nano Structured Coatings Institute, Yazd Payame Noor University, P. O. Box 89431-74559, Yazd, Iran

[3] Department of Physics, Payame Noor University, P.O. Box 119395-3697, Tehran, Iran

In metal elements, binding between transition metals and hydrogen molecule results from Kubas interaction, which emanates from the hybridization between H_2 molecule σ^* antibonding orbital and d orbitals of transition metals [17, 18]. The binding energy between H_2 molecule and TM is about 0.4 eV, which is suitable for the storage of hydrogen [15]. These metals, however, tend to accumulate on the graphene surface, which reduces the storage capacity of hydrogen [19]. Studies have shown that the formation of pores not only prevents the accumulation of intermediate metals on the graphene surface but also creates greater binding sites for the hydrogen molecule leading to its increased storage capacity [19–21].

Due to the benefits of intermediate metal atoms and the role of pores in graphene, it has been used to improve hydrogen storage. Several studies have been conducted in this regard. Yuan et al. [21] reviewed Y decoration on PG through the evaluation of adsorption energy using the CASTEP code. The hydrogen molecule could be absorbed around an atom of Y with an average energy of − 0.297 eV. Chen et al. [9] studied hydrogen storage on SC-PG based on DFT calculations. For a Sc atom, the most stable place is the center of the hexagonal carbon ring. Hydrogen can be absorbed around a Sc atom, with a mean binding energy of − 0.429 eV. The ability to absorb hydrogen molecules on Ti-PG has been studied recently. Ti atom was placed over the center of hexagonal carbon ring, so that Ti could highly be adsorbed on PG. Four hydrogen molecules around Ti atom were absorbed with a mean absorption energy of − 0.457 eV [16].

In the present study, the problem was improved by choosing the topology defect that holds the symmetry in a single layer of graphene and evaluates the hydrogen molecule adsorption. The structure was made by changing the size of this topological defect to keep the symmetry. The most stable adsorption site of Sc atoms is determined on four different sizes of PG by considering the mode of action of Sc-PG interplay. Subsequently, a discussion is presented on the adsorption ability of H_2 molecule on Sc-decorated PG system, followed by comparing the storage capacity and the adsorption mechanism of these four PGs. Eventually, the adsorption energy of H_2 molecules on PGs in the absence of Sc is examined for further understanding of Sc atom impacts.

Calculation details

All calculations were done utilizing the FHI-aims code. FHI-aims was programmed and set up to allow efficient all-electron calculations for any system type. The generalized gradient approximation (GGA) and PBE function were used to calculate the energy. The polarized spin calculations) collinear) were done in this work, along with using the light settings for all calculations. The entire atoms will be able to relax in all calculations, along with full optimization of the whole structure. The computational unit cell comprises a 5 × 5 of graphene cell with a vacuum of 15 Å. The periodic boundary conditions are applied to calculate the PG unit cell. Based on Tkatchenko and Scheffler, van der Waals (vdW) correction was used to investigate the role of vdW interaction in all computations by the use of a 5 × 5 × 1 k-point mesh. The Pulay algorithm was used to improve the relative ZORA approximation and to achieve a fast and stable convergence in the self-consistent cycle. A Gaussian occupation broadening was selected with a width of 0.05 eV.

Convergence criteria of 10^{-5}eV for the electron density, 10^{-3}eV for the eigenvalues, and 10^{-6} eV were applied for total energy of the system. The adsorption energies of Sc atom on PG structures are obtained by Eq. (1):

$$\overline{E}_b = [\, E_{\mathrm{Sc+PG}} - E_{\mathrm{PG}} - \mathrm{n}E_{\mathrm{Sc}} \,]/n \tag{1}$$

where $E_{\mathrm{Sc+PG}}$, E_{PG}, and E_{Sc} are total energies of the system with Sc atoms, PG layer, and a free Sc atom, respectively, and n is the number of adsorbed Sc atoms. The adsorption energy and mean adsorption energy of each H_2 molecule on Sc-decorated PG system are calculated by

$$E_{ab} = \left[E_{i\mathrm{H}_2+\mathrm{Sc+PG}} - E_{(i-1)\mathrm{H}_2+\mathrm{Sc+PG}} - E_{H_2}\right] \tag{2}$$

$$\overline{E}_{ab} = [E_{i\mathrm{H}_2+\mathrm{Sc+PG}} - E_{sc+\mathrm{PG}} - iE_{\mathrm{H}_2}]/i \tag{3}$$

where $E_{\mathrm{iH}_2+Sc+PG}$, $E_{(i-1)\mathrm{H}_2+Sc+PG}$, and E_{H_2} are total energies of the system with i H_2 molecules adsorbed, the $(i-1)$ H_2 molecules adsorbed, and free H_2 molecule, respectively. PG has two types of carbon atoms, C_1 and C_2, the former is connected to two carbons and one hydrogen atom, and the latter is linked to three carbon atoms. The bond distances of C_1–H, C_2–C_2 and C_1–C_2 are 1.085, 1.427, and 1.395 Å, respectively. Our results are in agreement with those of Li [22], who reported observations with GGA-PW91 function using DMol platform, indicating that our computational results are reliable.

Results and discussion

Electronic structure of Sc-decorated PG

Initially, the adsorption of Sc atom was considered on four different sizes of PG. According to Fig. 1, h_1, h_2, b_1, b_2, t_1, and t_2 are six sites for adsorption of a Sc atom on PGs, namely the center of C ring, the center of a half C ring, the bridge of C_1–C_2 bond, the bridge of C_2–C_2 bond, the top of C_1 atom, and the top of C_2 atom, respectively. Examination of the adsorption energies for different positions of the Sc atom on PGs reveals that the center of a hexagonal ring (h1) is the preferred adsorption site for a Sc atom on PGs.

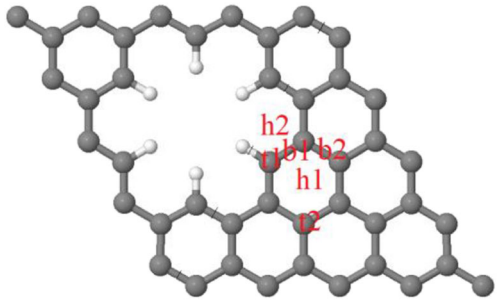

Fig. 1 Six primary absorption sites for a Sc atom on PG1. Gray and white balls indicate C and H atoms

Table 1 Mulliken population analysis of Sc atom on PG_1, PG_2, PG_3, and PG_4 structures

	Charge	*s*	*p*	*d*
Sc	0	8	12	1
PG_1-Sc	0.685	6.31	12.18	1.75
PG_2-Sc	0.679	6.32	12.18	1.74
PG_3-Sc	0.706	6.28	12.18	1.76
PG_4-Sc	0.709	6.3	12.18	1.74

The configuration in the presence of Sc atom after relaxation is displayed in Fig. 2. Accordingly, the position of Sc atom is slightly deformed with respect to the center of the C ring, with adsorption energies of − 2.654, − 2.693, − 2.909, and − 2.696 eV for a Sc atom on PG_1, PG_2, PG_3, and, PG_4, respectively.

The adsorption energy of Sc atom on pure graphene was also calculated to explain the effect of pores in graphene layer on the adsorption of Sc atom. The adsorption energy of Sc atom on 5 × 5 supercell of graphene is − 1.892 eV, which corresponds to that of Chen [23]. The adsorption energy of Sc atom on PGs is clearly higher than that of Sc atom on pure graphene. Table 1 lists the analysis of Mulliken atomic populations for Sc atom on four PGs. It shows that the partial charge of the Sc atom are donated from the 4s orbital to the PGs, which increases the negative charge of carbon and forms an electric field between Sc and PG layers. This results in back donations part of the charge from PG to the 3d orbital of Sc atom via hybridizations between C and Sc atoms. Increasing the pore size is associated with rising the amount of charge transfers from Sc atom.

The partial densities of states (PDOS) of Sc atom and C atom of Sc-PG system were examined to realize well the interplay between Sc atom and PGs. For all considered systems (Fig. 3), there is overlap between C 2p and Sc 3d orbitals around Fermi level, which indicates a robust hybridization between C and Sc atoms. Consequently, the polarization and the hybridization can contribute to Sc adsorption. Figure S1 depicts the band structures for all PGs in Supporting Information. PG_1 has almost the same electronic structure as graphene, and Dirac cones are at the k-points in both structures. PG_2 disturbs Dirac points, and Dirac cone forms at the M-point; therefore, the electronic structure of PG_2 is different from that of graphene. PG_3 and PG_4 break the lattice symmetry of pure graphene, and a band gap is formed at the Dirac point. For PG_3, the Fermi level is the middle of the band gap, which shifts toward the valence band for PG_4. It is also seen that the adsorption of Sc atom results in an n-type doping of the PGs in which the Fermi level shifts toward the conduction band.

Subsequently, the states of second Sc atoms adsorbed on PG structures are considered to study the accumulation of Sc atoms. Analysis of the energy indicates that the most preferable adsorption position is the center of C hexagon on the perimeter of PGs. As revealed by the present computations, the binding energy of the second Sc atom for all PG structures is stronger than the first one, resulting from the electric field stimulated by the first Sc atom. However, the cohesive energy of the Sc atom is greater than its binding energy on PGs, and the two Sc atoms lie closely to one another. This may be a trend of clustering among Sc atoms; therefore, only one Sc atom on PGs on the single side should be studied to avoid the clustering of Sc atoms.

Adsorption of H_2 molecules on Sc-decorated PGs

The capacity of hydrogen storage for Sc decorated on PG_1, PG_2, PG_3, and PG_4 is discussed here. The first H_2 molecule favors adsorption on the bridge of C–C bond as shown in Fig. 4. In Table 2, the adsorption energies of the first H_2 molecule of the four structures are − 0.568, − 0.553, − 0.509, and − 0.566 eV, respectively. Besides, the bond distance of H–H is extended from 0.753 Å of the isolated molecule to the

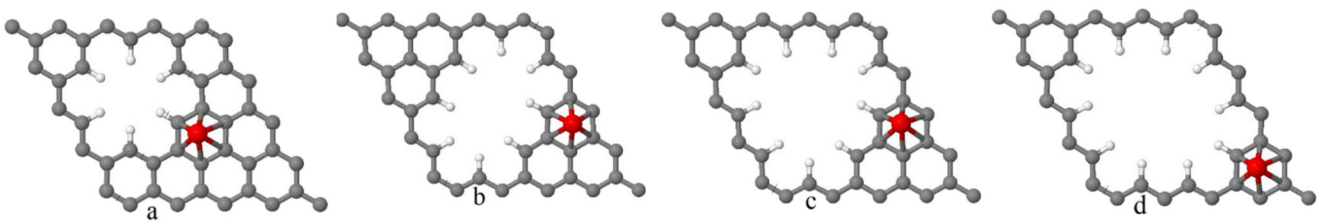

Fig. 2 The optimized geometry structure of a Sc atom–decorated PGs. (a) Sc-PG_1, (b) Sc-PG_2, (c) Sc-PG_3, and (d) Sc-PG_4. Gray, white, and red balls are C, H, and Sc atoms, respectively

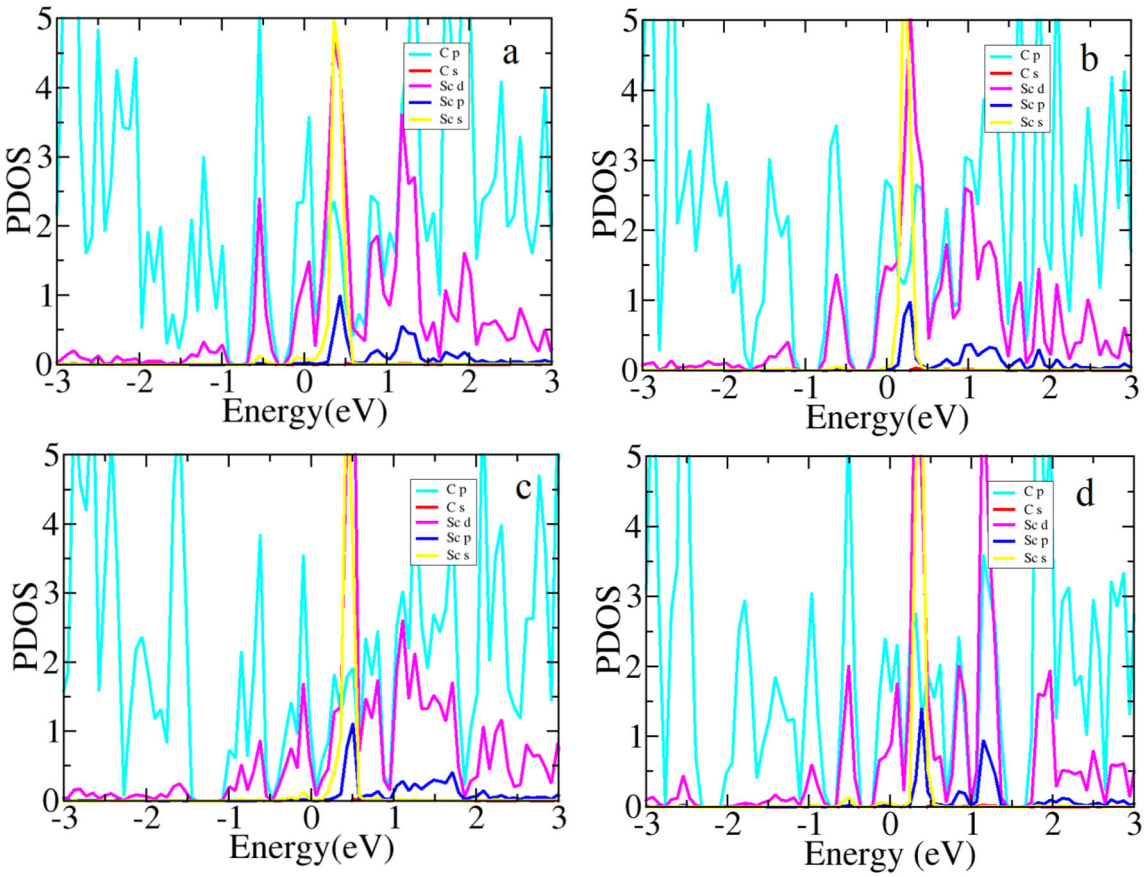

Fig. 3 PDOS of Sc (s, p, and d orbitals) and C (s and p orbitals) atoms in the system of Sc atom adsorbed on (a) PG1, (b) PG2, (c) PG3, and (d) PG4. The Fermi level was fixed to 0

range of 0.830–0.838 Å [18], indicating a robust adsorption of H_2 on Sc-PGs system.

Analyses of charge density difference, partial density of states, adsorption energy of PGs, and Sc-decorated PG system with one H_2 adsorbed are performed to examine the impact of Sc atom on the adsorption of H_2 molecule. The charge transfers of the PG and Sc-PG systems are observable via charge density difference ($\Delta\rho$), so $\Delta\rho$ is presented as

$$\Delta\rho = \rho_{iH_2+PG} - \rho_{iH_2} - \rho_{PG} \quad (4)$$

$$\Delta\rho = \rho_{iH_2+Sc+PG} - \rho_{iH_2} - \rho_{Sc+PG} \quad (5)$$

where $\rho_{iH_2+Sc+PG}$, ρ_{iH_2+PG} , ρ_{iH_2}, ρ_{Sc+PG}, and ρ_{PG}denote the charge density of the total Sc-PG system, the charge density of total PG system, the charge density of i adsorbed H_2 molecules, the charge density of Sc-decorated PG system, and the charge density of PG system, respectively. The charge density difference of the first H_2 molecule adsorbed on PG structures is displayed in Fig. 5, where the blue and red colors denote electron accumulation and depletion sites, respectively. For Sc-PG systems, Fig. 5(a) depicts a clear charge accumulation between H_2 molecules and Sc atom. In addition, charge depletion and accumulation observed at either side of the H_2 molecule indicate the polarization of H_2 molecule, thereby raising the H_2-PG interplay because of the Kubas interaction [18, 24–27]. Values for the isosurface of the four structures are 0.006, 0.007, 0.007, and 0.007 e/Å3, respectively. The charge density difference of the first H_2 molecule adsorbed on PGs without the presence of Sc atom (Fig. 5(b)) indicates that the charge distribution is nearly on the pore center and the

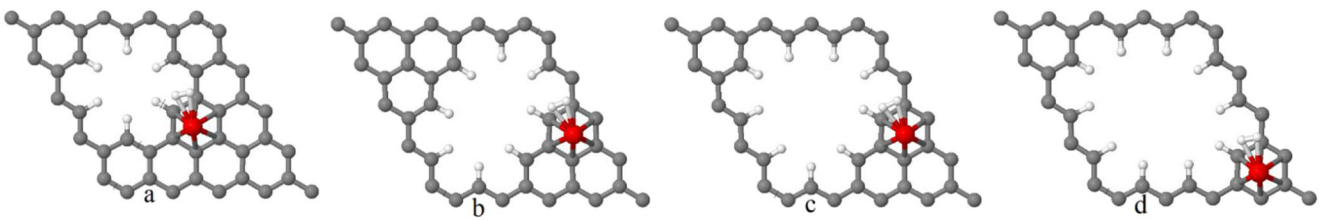

Fig. 4 Optimized geometries of a Sc atom–decorated PGs with one H_2 adsorbed there on. (a) PG1, (b) PG2, (c) PG3, and (d) PG4, respectively

Table 2 Estimated binding energies and bond distances of one hydrogen molecule adsorbed on Sc-decorated PG_1, PG_2, PG_3, and PG_4, respectively

Name	Eab (eV)	dH-H (Å)
PG_1-H_2	− 0.568	0.830
PG_2-H_2	− 0.553	0.833
PG_3-H_2	− 0.509	0.838
PG_4-H_2	− 0.566	0.830

isosurface has a value of about 0.000 e/Å3 for all the structures. Furthermore, from Fig. 5(a), it is seen that the existence of Sc atom causes the accumulation of charge on the perimeter of pores.

From PDOS of the first H_2 molecule adsorbed on PGs and Sc-decorated PG system (Fig. 6) and the Supporting Information (Figs. S2, S3, and S4) for all the PGs, it can be observed that H_2 molecule in PG system has a weak interaction because there is no overlap between H_2 and PGs. In Sc-decorated PG systems, on the other hand, several overlaps exist in the main peaks of $H_2$1s, Sc3d, and C2p orbitals around the Fermi level, suggesting strong interactions between H_2, Sc, and PGs. Among all possible structures, PG_3 has a weak interaction with H_2 molecule because of small sharp peaks around the Fermi level. Figure 7 displays the adsorption energy of the first H_2 on Sc-PGs and that of the first H_2 on PGs without the presence of Sc atom. The binding energies for Sc-PG system ranges from 0.2 to 0.7 eV/H_2 fulfilling the necessity that H_2 molecule is capable of adsorption and desorption under surrounded settings [28]. In addition, the adsorption energy of the first H_2 on PG_3 is less than that of PG_1, PG_2, and PG_4, as displayed in Fig. 8(a). The adsorption energy of PGs without the presence of Sc atom is not in the desirable range (Fig. 8(b)). Therefore, the existence of Sc atom would reinforce the adsorption energy of H_2 molecule on PGs.

Figure 8 presents the post-relaxation configuration for PG_1 in the event of extra H_2 molecules adsorption on Sc-PG structure. For the adsorption of H_2 on Sc-decorated PG_2, PG_3, and

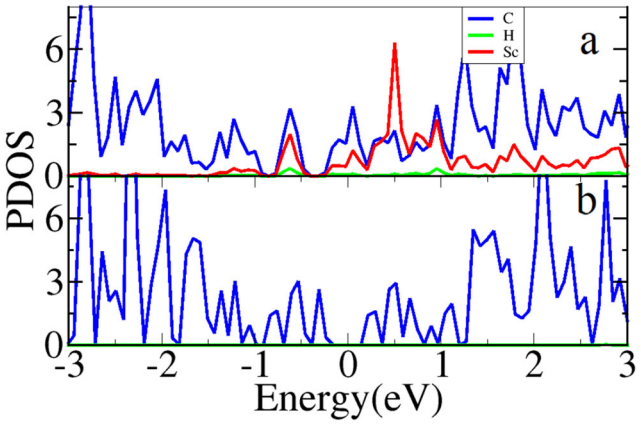

Fig. 6 PDOS for H_2 1s (green line), Sc 3d (red line), and C2p (blue line) orbitals when one H_2 molecule is adsorbed on (a) Sc-PG_1 and (b) PG_1 without the presence of Sc atom. The Fermi level is located at 0

PG_4, the optimized geometries resemble that on Sc-decorated PG_1. H_2 molecules prefer symmetrical absorption around Sc atom. As shown in Fig. 8, the first four H_2 molecules are bonded to Sc atom, and the fifth H_2 molecule moves to an upper layer without forming a bond with Sc atom. Furthermore, the adsorption energies of the fifth H_2 molecule on PGs are − 0.167, − 0.114, − 0.159, and − 0.169 eV, respectively, being incapable for hydrogen storage uses [29]. Hence, an uppermost number of four H_2 molecules are absorbable on Sc-PG system, and average adsorption energies for PG_1, PG_2, PG_3, and PG_4 are − 0.547, − 0.539, − 0.546, and − 0.553 eV/H_2, respectively, being higher than a mean adsorption energy of − 0.429 eV/H_2 reported by Chen [9] (Table 3).

Figure 9 displays the PDOS of H_2 1s and Sc 3d orbitals upon adsorption of 1–5 H_2 molecules on Sc-decorated PG_1. In addition, analysis of the PDOS of H_2 molecules on Sc-decorated PG_2, PG_3, and PG_4 demonstrates a similar adsorption behavior in all the four structures. It is obvious that the peaks of H_2 1s and Sc 3d orbitals overlap within − 10 to − 8 eV, suggesting a strong hybridization between orbitals of H_2

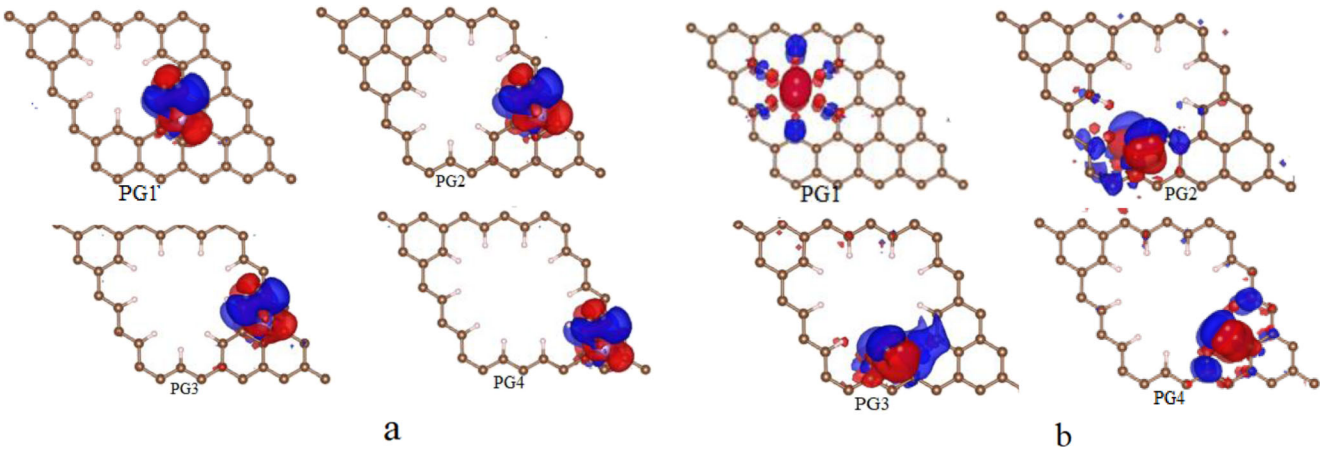

Fig. 5 The isosurfaces of charge density differences for one H_2 adsorption on PGs. The blue and red colors characterize electron accumulation and depletion sites. (a) Sc-decorated PGs with one adsorbed H_2 and (b) PGs with one adsorbed H_2

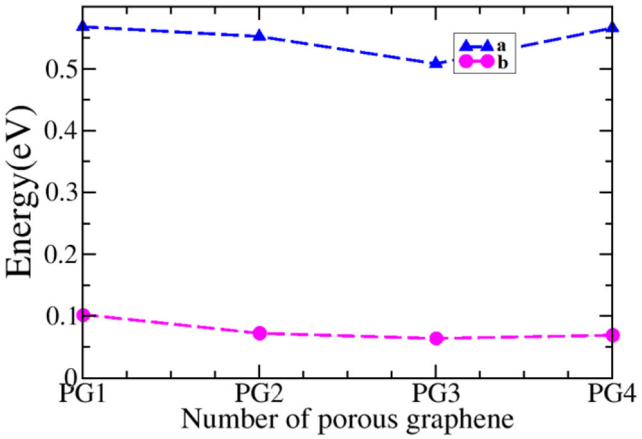

Fig. 7 Calculated binding of the first H_2 molecules on (a) Sc-decorated PGs and (b) on PGs without the presence of Sc atom

1s and Sc 3d. Furthermore, the adsorption of 1~4 H_2 molecules also reveals that there is a hybridization between H_2 and Sc atom around − 1 eV, which can be a reason for the lack of a strong interplay of the fifth H_2 molecule with Sc atom.

Figure 10 summarizes the adsorption energy of each H_2 molecule on PG_1, PG_2, PG_3, and PG_4 with rising number of H_2 molecules. It is observed that the adsorption energy of the second H_2 is greater than that of the first H_2, and the adsorption energy of the third H_2 is weaker than that of the forth H_2 on all the four structures. As this result is understood from PDOS (Fig. 9(a) and (b)), the band expansion of the H_2 molecular level below the Fermi energy (around − 9 eV) shows the interplay between H_2-H_2 molecules, which in turn could elevate the binding energies of the second H_2, being in full agreement with previous reports [30–32]. Additionally, analysis of the H–H bond length (Supporting Information in Table S1) can justify the relatively weak adsorption of the

Table 3 Absorption energies (ΔE), average adsorption energies ($\Delta \bar{E}$), bond lengths of hydrogen, and charges of Sc atom (Δq_{Sc}) on Sc-PG_1 system

No. of H_2	1	2	3	4	5
ΔE (eV)	− 0.568	− 0.612	− 0.438	− 0.571	− 0.167
$\Delta \bar{E}$ (eV)	− 0.568	− 0.59	− 0.539	− 0.547	− 0.471
Δq_{Sc}	0.632	0.429	0.257	0.065	− 0.09
d-H-H (Å)	0.830	0.831	0.796	0.814	0.754

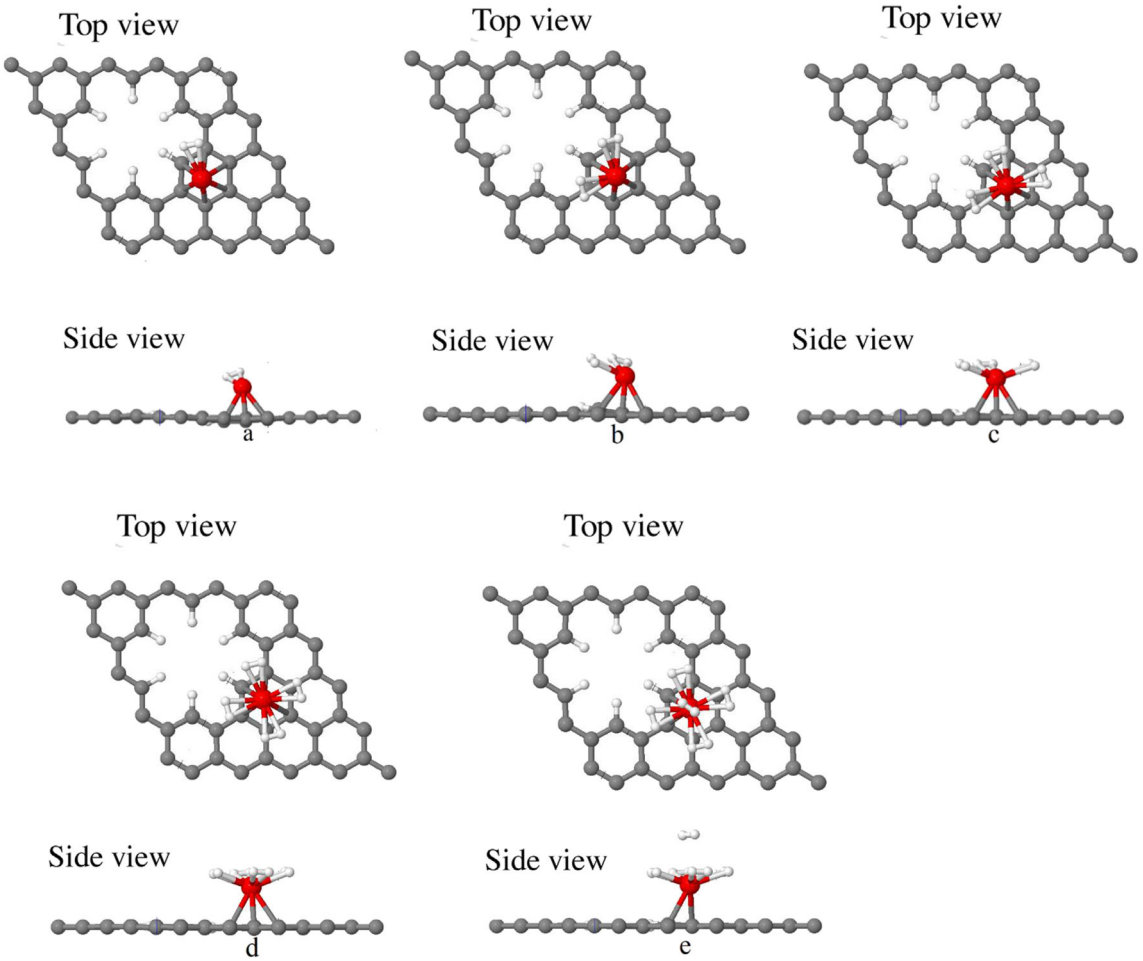

Fig. 8 Optimized atomic structure of Sc- PG_1 system with (a) one, (b) two, (c) three, (d) four, and (e) five hydrogen molecules attached

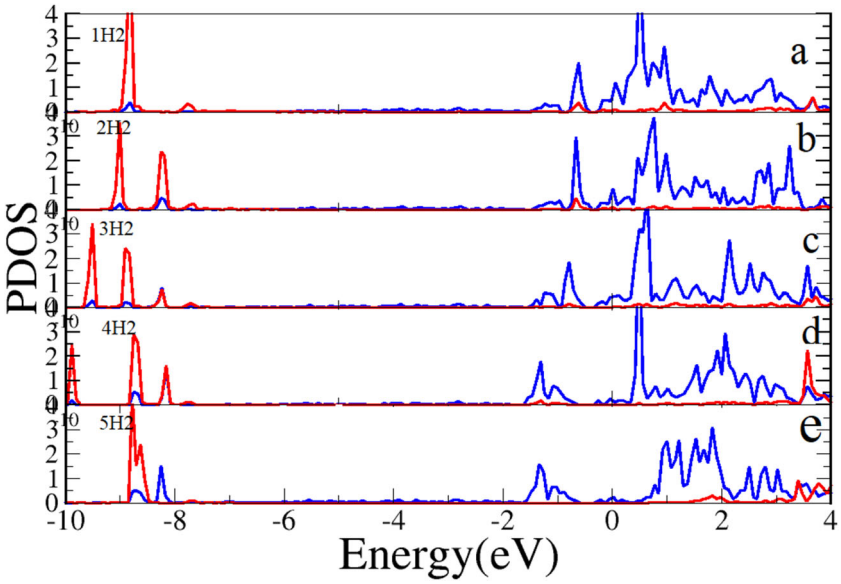

Fig. 9 PDOS of H_2 1s (red line) and Sc 3d (blue line) orbitals for adsorption of 1–5 H_2 molecules in Sc-PG_1. The Fermi level is fixed at zero

third H_2. Figure 9 also displays that the adsorption energy of H_2 molecules on Sc-decorated PGs (except for PG_1) rises regularly with growing the pore size, which may be due to the symmetry of PG structures. However, the binding energies of H_2 molecules on Sc-adorned PG_4 are uppermost among the four studied structures. Our calculations show that the system with a higher overlap around the Fermi level is suitable for hydrogen storage.

Conclusions

The adsorption of Sc atom on four different sizes of porous graphene and of H_2 molecules on Sc-decorated PG system were studied using FHI-aims code. A very slight deformation of PGs suggests that Sc atom prefers to be adsorbed on the central area over the C hexagon, and that Sc atom has a strong adsorption on PGs. Charge density difference, partial density of states, and adsorption energy were analyzed to examine the effect of Sc atom on the adsorption of H_2 molecule, showing that the presence of Sc atom would strengthen the adsorption energy of H_2 molecule on PGs. Four H_2 molecules are adsorbable around Sc atom for the single side of PGs. According to the analysis of the partial density of states, the adsorption of H_2 molecules on the PG systems is related to orbital hybridization among Sc, H, and C atoms, as well as to the polarization between Sc and H atoms. The mean adsorption energies of H_2 molecules on Sc-decorated PG_4 were uppermost among the four studied structures. Accordingly, the adsorption energy of H_2 molecules on Sc-adorned PG system rises steadily with increasing the pore size.

Acknowledgments This work was supported by the Vice Chancellor for Research Affairs of Payame Noor University. F. Yasareh appreciates Nano Structured Coatings Institute of Yazd Payame Noor University for financial support as well as computation resources during his studies.

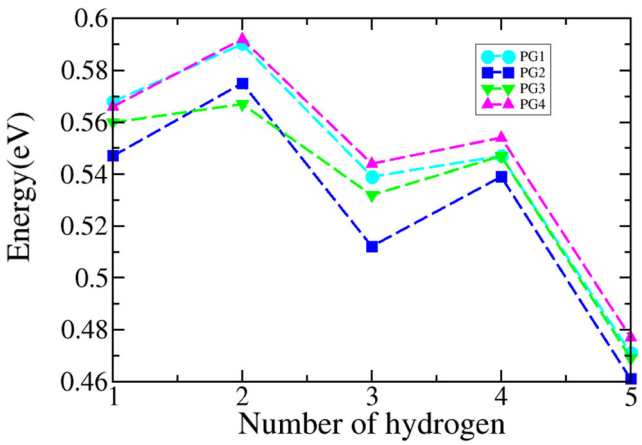

Fig. 10 A comparison of adsorption energies for five hydrogen molecules on four different sizes of porous graphene

References

1. Xia Y, Yang Z, Zhu Y (2013) Porous carbon-based materials for hydrogen storage: advancement and challenges. J. Mater. Chem. A 1:9365–9381
2. Berenguer-Murcia Á, Marco-Lozar JP, Cazorla-Amór D (2018) Hydrogen storage in porous materials: status, milestones, and challenges. Chem. Rec. 18:900–912
3. Ren J, Musyoka NM, Langmi HW, Mathe M, Liao S (2017) Current research trends and perspectives on materials-based hydrogen storage solutions: a critical review. Int J Hydrog Energy 42: 289–311
4. Tozzini V, Pellegrini V (2013) Prospects for hydrogen storage in graphene. Phys. Chem. Chem. Phys. 15:80–89

5. Ao Z, Dou S, Xu Z, Jiang Q, Wang G (2014) Hydrogen storage in porous graphene with Al decoration. Int J Hydrog Energy 39: 16244–16251
6. Niaz S, Manzoor T, Pandith AH (2015) Hydrogen storage: materials, methods and perspectives. Renew. Sust. Energ. Rev. 50:457–469
7. Wang F, Zhang T, Hou X, Zhang W, Tang S, Sun H, Zhang J (2017) Li-decorated porous graphene as a high-performance hydrogen storage material: a first-principles study. Int. J. Hydrog. Energy 42:10099–10108
8. Liu W, Liu Y, Wang R (2014) Prediction of hydrogen storage on Y-decorated graphene: a density functional theory study. Appl. Surf. Sci. 296:204–208
9. Chen Y, Wang J, Yuan L, Zhang M, Zhang C (2017) Sc-decorated porous graphene for high-capacity hydrogen storage: first-principles calculations. Materials 10:894
10. Yu X, Tang Z, Sun D, Ouyang L, Zhu M (2017) Recent advances and remaining challenges of nanostructured materials for hydrogen storage applications. Prog. Mater. Sci. 88:1–48
11. Lee H, Ihm J, Cohen ML, Louie SG (2010) Calcium-decorated graphene-based nanostructures for hydrogen storage. Nano Lett. 10:793–798
12. Li D, Wang C, Niu Y, Zhao H, Liang C (2014) Structural and electronic properties of MnO3 (4) super halogen clusters embedded in graphene. Chem. Phys. Lett. 601:16–20
13. Sivek J, Sahin H, Partoens B, Peeters FM (2013) Adsorption and absorption of boron, nitrogen, aluminum, and phosphorus on silicone: stability and electronic and phonon properties. Phys. Rev. B 87:085444
14. Vogt P, De Padova P, Quaresima C, Avila J, Frantzeskakis E, Asensio MC, Resta A, Ealet B, Le Lay G (2012) Silicene: compelling experimental evidence for graphene like two-dimensional silicon. Phys. Rev. Lett. 108:155501
15. Zhao H (2012) Strain and chirality effects on the mechanical and electronic properties of silicene and silicane under uniaxial tension. Phys. Lett. A 376:3546–3550
16. Yuan L, Kang L, Chen Y, Wang D, Gong J, Wang C, Zhang M, Wu X (2018) Hydrogen storage capacity on Ti-decorated porous graphene: first-principles investigation. Appl. Surf. Sci. 434:843–849
17. Shiraz HG, Tavakoli O (2017) Investigation of graphene-based systems for hydrogen storage. Renew. Sust. Energ. Rev. 74:104–109
18. Reunchan P, Jhi S-H (2011) Metal-dispersed porous graphene for hydrogen storage. Appl. Phys. Lett. 98:093103
19. He H, Chen X, Zou W, Li R (2018) Transition metal decorated covalent triazine-based frameworks as a capacity hydrogen storage medium. Int. J. Hydrog. Energy 43:2823–2830
20. Han S, Wu D, Li S, Zhang F, Feng X (2014) Porous graphene materials for advanced electrochemical energy storage and conversion devices. Adv. Mater. 26:849–864
21. Yuan L, Chen Y, Kang L, Zhang C, Wang D, Wang C, Zhang M, Wu X (2017) First-principles investigation of hydrogen storage capacity of Y-decorated porous graphene. Appl. Surf. Sci. 399: 463–468
22. Li Y, Zhou Z, Shen P, Chen Z (2010) Two-dimensional polyphenylene: experimentally available porous graphene as a hydrogen purification membrane. Chem. Commun. 46:3672–3674
23. Luo Z, Fan X, Pan R, An Y (2017) A first-principles study of Sc-decorated graphene with pyridinic-N defects for hydrogen storage. Int. J. Hydrog. Energy 42:3106–3113
24. Sun Q, Jena P, Wang Q, Marquez M (2006) First-principles study of hydrogen storage on Li12C60. J. Am. Chem. Soc. 128:9741–9745
25. Chandrakumar KRS, Ghosh SK (2008) Alkali-metal-induced enhancement of hydrogen adsorption in C60 fullerene: an ab initio study. Nano lett 8:13–19
26. Dimitrakakis GK, Tylianakis E, Froudakis GE (2008) Pillared graphene: a new 3-D network nanostructure for enhanced hydrogen storage. Nano letters 8:3166–3170
27. Ataca C, Akturk E, Ciraci S, Ustunel H (2008) High-capacity hydrogen storage by metallized graphene. Appl. Phys. Lett. 93: 043123
28. Zhang Z, Li J, Jiang Q (2010) Hydrogen adsorption on Eu/SWCNT systems: a DFT study. J. Phys. Chem. C 114:7733–7737
29. Bhattacharya A, Bhattacharya S, Majumder C, Das GP (2010) Transition-metal decoration enhanced room-temperature hydrogen storage in a defect-modulated graphene sheet. J. Phys. Chem. C 114:10297–10301
30. Ataca C, Aktürk E, Ciraci S (2009) Hydrogen storage of calcium atoms adsorbed on graphene: first-principles plane wave calculations. Phys Rev B 79:041406
31. Ao ZM, Peeters FM (2010) High-capacity hydrogen storage in Al-adsorbed graphene. Phys. Rev. B 81:205406
32. Chen M, Yang X-B, Cui J, Tang J-J, Gan L-Y, Zhu M, Zhao Y-J (2012) Stability of transition metals on Mg (0001) surfaces and their effects on hydrogen adsorption. Int J Hydrog Energy 37:309–317